# Characterization of a state-insensitive dipole trap for cesium atoms

P. Phoonthong, P. Douglas, A. Wickenbrock, and F. Renzoni
*Department of Physics and Astronomy, University College London, Gower Street, London WC1E 6BT, United Kingdom*
(Received 7 April 2010; published 12 July 2010)

In this work we characterize a state-insensitive dipole trap for cold cesium atoms, as realized by tightly focusing a single running laser beam at the magic wavelength. The use of trapping light at the magic wavelength of 935.6 nm resulted in the same ac Stark shift for the $^6S_{1/2}$ ground state and the $^6P_{3/2}$ excited state. A complete characterization of the trap is given, which includes the dependence of the lifetime on the trap depth, an analysis of the important role played by a depumper beam, and a comparison with dipole trapping at different (nonmagic) wavelengths. In particular, we measured the differential light shift of the relevant optical transition as a function of the trapping light wavelength, and showed that it becomes zero at the magic wavelength. Our results are compared to previous realizations of state-insensitive dipole traps for cesium atoms. We also discuss the possible role of the state-insensitive trap, its limitations, and possible developments for the study of ground-state quantum coherence phenomena and related applications.

DOI: 10.1103/PhysRevA.82.013406 PACS number(s): 37.10.−x, 42.50.−p

## I. INTRODUCTION

Far-detuned optical dipole traps (FORTs) [1] are a basic tool in many cold atom experiments. They allow confinement of cold atoms with long storage times and they can be combined with evaporative cooling to produce Bose-Einstein condensates directly in the dipole trap.

Dipole traps rely on the spatial variation of the ac Stark shift of atomic levels, as typically obtained by spatially varying the intensity of the trapping beam. In general, different atomic levels have different polarizabilities and thus experience different ac Stark shifts. This can be a severe limiting factor for applications in metrology, as the spatial modulation of the state-dependent ac Stark shift results in a broadening of the atomic transition. Also, the spatial modulation of the transition frequencies does not allow the direct use of the cooling techniques developed for free-space applications. These limitations can be overcome with the use of state-insensitive dipole traps, which have been recently proposed and demonstrated [2–8].

State-insensitive dipole traps take advantage of the multilevel structure of the atom of interest. For a given transition, the ac Stark shifts of the ground and excited state are not given only by the interaction of the far-detuned field with that transition, but are determined by the interaction of the detuned beam with all transitions of the multilevel atomic structure. Thus it is possible, at least for certain atomic species, to choose the wavelength of the laser field so that the resulting ac Stark shifts of the ground and excited state of the transition of interest are equal; that is, the differential ac Stark shift of such a transition is zero, and state-independent trapping can be realized. The appropriate wavelength is usually termed the *magic* wavelength.

Magic wavelength dipole traps have been developed for essentially two different purposes. The main application is in frequency standards. The elimination of the differential ac Stark shifts for the "clock transition" allows the use of trapped atoms for the realization of atomic clocks. For clock transitions in the optical domain, atomic clocks with atoms in state-insensitive traps have been demonstrated [3–5]. For the microwave transition of cesium primary standards, purely optical magic wavelengths have been shown not to exist [9]. However, the application of an appropriate magnetic field may lead to the cancellation of the relevant differential light shift [10]. For other elements, such as Ga and Al, the magic wavelength for microwave transitions exists also in the absence of an applied magnetic field [11]. A second application, of interest for the present work, relies on state-independent traps to be able to optically address *trapped* atoms as if they were free. In particular, this allows one to use free-space laser-cooling techniques for trapped atoms and to precisely address a given optical transition, as required in most applications in quantum optics, without having to detune the lasers to compensate for the differential light shift and without the broadening due to the spatial variation of the laser intensity.

In this work we characterize a state-insensitive dipole trap for cold cesium atoms, as realized by tightly focusing a single running laser beam at the magic wavelength. The use of trapping light at the *magic* wavelength of 935.6 nm resulted in the same ac Stark shift for the $^6S_{1/2}$ ground state and the $^6P_{3/2}$ excited state. A complete characterization of the trap is given, which includes the dependence of the lifetime on the trap depth, an analysis of the important role played by a depumper beam, and a comparison with dipole trapping at different (nonmagic) wavelengths. In particular, we measured the differential light shift of the relevant optical transition as a function of the trapping light wavelength, and showed that it becomes zero at the magic wavelength. Our results are compared to previous realizations of state-insensitive dipole traps for cesium atoms [6,7]. We also discuss the possible role of the state-insensitive trap, its limitations and possible developments, for the study of ground-state quantum coherence phenomena, and related applications.

This work is organized as follows. In Sec. II we describe the experimental setup. In Sec. III we characterize our dipole trap. In particular, we studied the dependence of the lifetime on the trap depth, and analyzed the role of the depumper. Measurements of the differential light shift of the relevant optical transition as a function of the trapping light wavelength are also presented. The state-insensitive nature of the trap is verified and the relevant loss mechanisms are identified. Section IV concludes and summarizes our work.

 

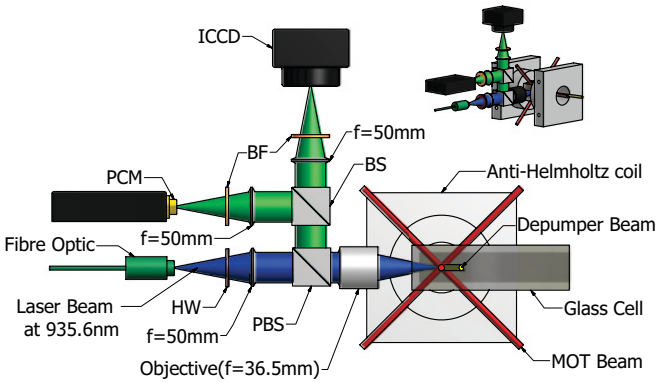


FIG. 1. (Color online) Sketch of the experimental setup. ICCD is an intensified charge-coupled device camera, PCM a photon-counting module, BF a band pass filter, (PBS) BS a (polarizing) beam splitter, and HW a half-wave plate.

## II. EXPERIMENTAL SETUP

A sketch of the experimental setup is shown in Fig. 1.

A magneto-optical trap (MOT) for cesium atoms is formed inside a glass cell. The cell, made of fused silica, has external dimensions of $30 \times 30 \times 100$ mm, and a glass thickness of 5 mm. Dispensers are used as a source of cesium atoms, so as to have an excellent vacuum within our single cell setup. The MOT is a standard six beam setup operating on the $D_2$ line, with the cooling light tuned to the red of the $F_g = 4 \rightarrow F_e = 5$ transition, and the repumper beam tuned to the $F_g = 3 \rightarrow F_e = 4$ transition. Our setup also includes a *depumping* beam, tuned to the $F_g = 4 \rightarrow F_e = 3$ $D_2$-line transition. Once the MOT beams have been switched off, the application of the depumping beam allows us to prepare a wanted fraction of the atoms in the $F_g = 3$ ground state. In this respect, it should be noticed that merely switching off the repumper during the MOT operation is not sufficient to pump the entire atomic population into the $F_g = 3$ sublevel owing to the large excited-state hyperfine splitting of cesium [12].

The linearly polarized dipole trap beam is generated by a Ti:sapphire laser (Coherent MBR-110 pumped by a Verdi V8). The laser is tuned to the wavelength $\lambda = 935.6$ nm. This is the magic wavelength for cesium atoms, for which the $^6S_{1/2}$ ground state and the $^6P_{3/2}$ excited state experience the same ac Stark shift. The beam is transported near the cell using an optical fiber, and tightly focused on the atomic cloud using a large numerical aperture objective. The objective, with a focal distance of $f = 43.6$ mm, is made of four lenses, and follows the design of Ref. [13]. We made direct measurements of the waist of the focused beam as transmitted through a single glass window of the same material as the glass cell. We measured a waist size $w_0 = (6.69 \pm 0.05)$ $\mu$m.

The typical experimental sequence is as follows. The MOT is loaded from the background vapor for 5 s. Such a relatively long loading time is needed as the cesium dispensers are run at a low current so as to have a low cesium background pressure. This is an essential requirement for a long lifetime of the dipole trap. After the MOT loading phase, the dipole-trap beam is turned on. It will be left on for the whole experimental sequence, including during the imaging phase. Simultaneously with the turning on of the dipole-trap beam, the MOT cooling beam detuning $\Delta$ and magnetic-field gradient $\nabla B$ are increased linearly, over 10 ms, from their initial values $\Delta = -2.5\Gamma_{3/2}$ and $\nabla B = 22.5$ G/cm to their final values $\Delta = -4\Gamma_{3/2}$ and $\nabla B = 30$ G/cm. Here $\Gamma_{3/2}$ is the width of the $6\,^2P_{3/2}$ excited state. Then the MOT and dipole trap are left simultaneously on for 50 ms. Finally the MOT beams and magnetic field are turned off and the atoms are left in the dipole trap for a variable "trapping time" $\Delta t$. For the measurements in which it is required, a depumping beam, with waist 4.7 mm and variable intensity $I_{\mathrm{dep}}$, is also applied during the trapping time $\Delta t$. For the imaging, we turn back on the MOT beams (but not the magnetic field) and after 4 ms an image is taken with the charge-coupled device (CCD) camera, with a typical integration time of also 4 ms.

## III. CHARACTERIZATION

### A. Trap frequencies

A single focused laser beam leads to three-dimensional trapping [1]. For atoms trapped near the bottom of the well the resulting potential can be written as

$$U(r,z) \simeq U_0\left[1 - 2\left(\frac{r}{w_0}\right)^2 - \left(\frac{z}{z_R}\right)^2\right], \tag{1}$$

where $z$ is the light propagation axis and $r$ the radial one; $z_R$ is the Rayleigh length $z_R = \pi w_0^2/\lambda$. The trap depth $U_0$ can be determined from the trapping beam intensity by including the contributions to the ground-state ac Stark shift from both $D_1$ and $D_2$ lines:

$$U_0 = \frac{\pi c^2}{2}\left(\frac{2\Gamma_{3/2}}{\omega_{3/2}^2\Delta_{3/2}} + \frac{\Gamma_{1/2}}{\omega_{1/2}^2\Delta_{1/2}}\right) I_0. \tag{2}$$

Here $\Gamma_{1/2}$ and $\Gamma_{3/2}$ are the widths of the $6\,^2P_{1/2}$ and $6\,^2P_{3/2}$ excited states, respectively. The angular frequencies $\omega_{1/2}$ and $\omega_{3/2}$ are the transition frequencies for the $D_1$ ($6\,^2S_{1/2} \rightarrow 6\,^2P_{1/2}$) and $D_2$ ($6\,^2S_{1/2} \rightarrow 6\,^2P_{3/2}$) lines, respectively. $I_0$ is the trapping beam intensity which can be expressed in terms of the beam power $P$ and the beam waist $w_0$ as

$$I_0 = \frac{2P}{\pi w_0^2}. \tag{3}$$

In the limit where Eq. (1) holds (i.e., for atoms sufficiently cold so that they explore only the bottom of the potential well), the trapping potential can be characterized by the radial ($\omega_r$) and the axial ($\omega_z$) oscillation frequencies,

$$\omega_r = \sqrt{\frac{-4U_0}{m w_0^2}}, \tag{4a}$$

$$\omega_z = \sqrt{\frac{-2U_0}{m z_R^2}}. \tag{4b}$$

We measured the vibrational frequencies by using the method of parametric heating [1,14]. We modulated the intensity of the trapping beam at a frequency $\omega$. Whenever $\omega = 2\omega_{r,z}/n$, with $n$ an integer, the atoms are heated up and expelled from the trap. Thus, the vibrational frequencies can be determined by measuring the number of atoms left in the trap as a function of the modulation frequency. A more sensitive

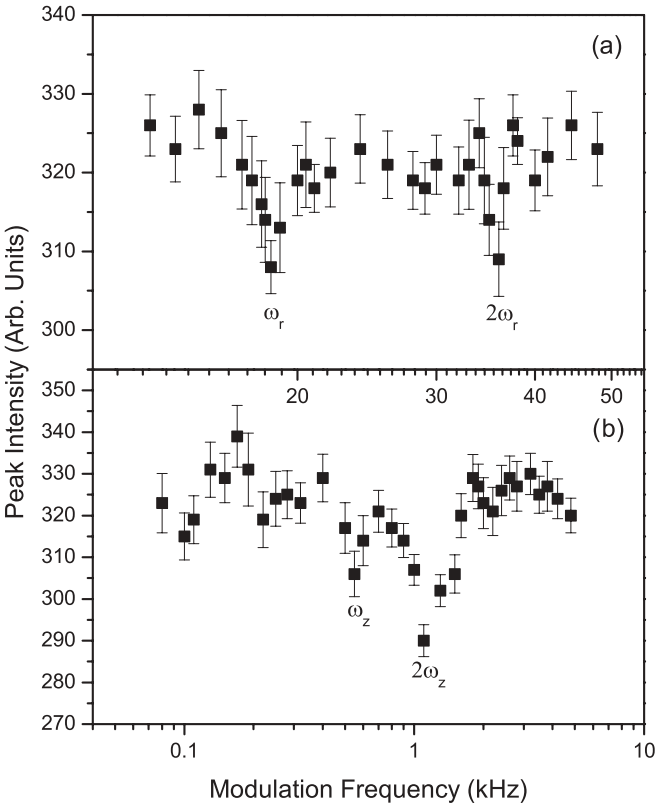


FIG. 2. Excitation spectra of Cs atoms trapped in a dipole trap at the magic wavelength. The peak fluorescence intensity from the trapped atomic sample is reported as a function of the trapping beam modulation frequency. The trapping beam power was $P = (254 \pm 2)$ mW for the data in (a) and $P = (231 \pm 1)$ mW for the data in (b). The beam power modulation amplitude was 50% for frequencies up to 500 Hz and 15% for frequencies larger than 500 Hz.

method consists of measuring the peak density (i.e., the peak intensity of the recorded fluorescence), rather than the total number of trapped atoms [15]. This is the method we adopted. The results of our measurements are shown in Fig. 2, where for both the longitudinal and radial frequency a decrease in peak density is observed for excitation at the fundamental frequency ($\omega = 2\omega_r$ and $\omega = 2\omega_z$) as well as for the excitation at the first subharmonic ($\omega = \omega_r$ and $\omega = \omega_z$). From the presented data, we derive the following: $\omega_r/(2\pi) = (18.5 \pm 0.1)$ kHz, $\omega_z/(2\pi) = (550 \pm 10)$ Hz. From each of these frequencies, and from the measured laser power, we can derive via Eqs. (2), (3), and (4) a value for the beam waist $w_0$. We derived $w_0 = (6.63 \pm 0.04)$ $\mu$m from the value for $\omega_r$ and $w_0 = (6.67 \pm 0.02)$ $\mu$m from the value for $\omega_z$. These values are consistent with the value $w_0 = (6.69 \pm 0.05)$ $\mu$m obtained by direct measurement of the beam waist, with the glass cell replaced by a window of the same material.

### B. Trap lifetime

An important parameter of the dipole trap is its lifetime. Previous work on far-detuned traps at 1064 nm for cesium atoms showed that the lifetime of the trapped atoms depends significantly on the atomic state [16]. For atoms prepared in the lower hyperfine ground state $F = 3$ a long lifetime was

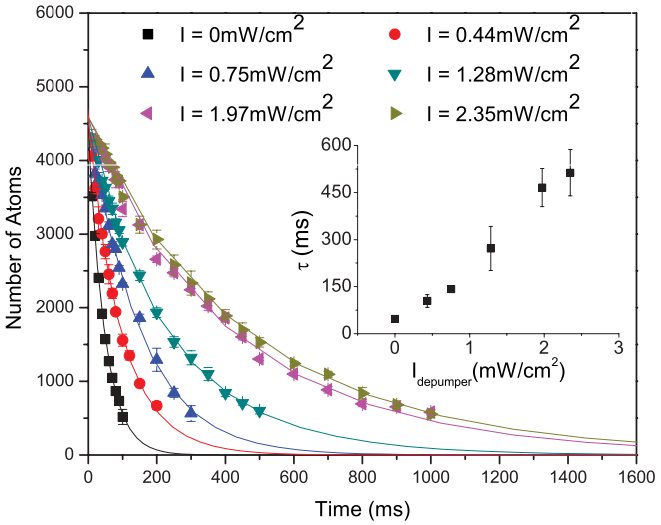


FIG. 3. (Color online) Atom number decay curves for different values of the depumper intensity. The lines are best fits of the data with the solution of Eq. (5). The trap lifetime, as derived from the fit of the decay curves, is shown in the inset as a function of the depumper intensity. The trap depth is $U_0/k_B = -1.78$ mK for all reported measurements.

observed as the dominating loss mechanism are collisions with the background gas. Instead, for atoms prepared in the upper hyperfine ground state $F = 4$, hyperfine-changing collisions are the dominating loss mechanism, and a much shorter lifetime was observed. As the same behavior is expected in our dipole trap, we studied the number of atoms in the trap versus time for different values of the intensity of the applied depumping beam.

We fitted our decay curves for the number $N$ of trapped atoms with the solution of the equation

$$\frac{dN}{dt} = -\Gamma N - \beta' N^2, \tag{5}$$

which is known to well describe the dynamics of the atoms in a far-detuned dipole trap [17]. The fitting parameters are $N_0$, the initial number of trapped atoms, $\Gamma$, the exponential loss rate, and $\beta'$, the atom number collisional loss coefficient. From the derived value of $\Gamma$ we also derive the trap lifetime $\tau = 1/\Gamma$. The results of our measurements, reported in Fig. 3, clearly show that the application of a depumping beam leads to an increase in the trapped atoms' lifetime. This is in agreement with the previous results mentioned earlier, as the application of a depumper leads to the preparation of atoms in the $F_g = 3$ ground state.

As the role of the depumping beam is to prepare a fraction of atoms in the $F_g = 3$ ground-state sublevel, a saturation effect is to be expected when the intensity of the depumper is large enough to prepare essentially all atoms in the wanted state. This was verified by measuring the number of atoms left in the trap after a fixed trapping time $\Delta t = 100$ ms, for a variable depumper intensity. The results of these measurements, presented in Fig. 4, clearly show the expected saturation effect: the number of atoms left in the trap increases with the depumper intensity and then becomes constant at $I_{\mathrm{dep}} \simeq 2$ mW/cm$^2$.

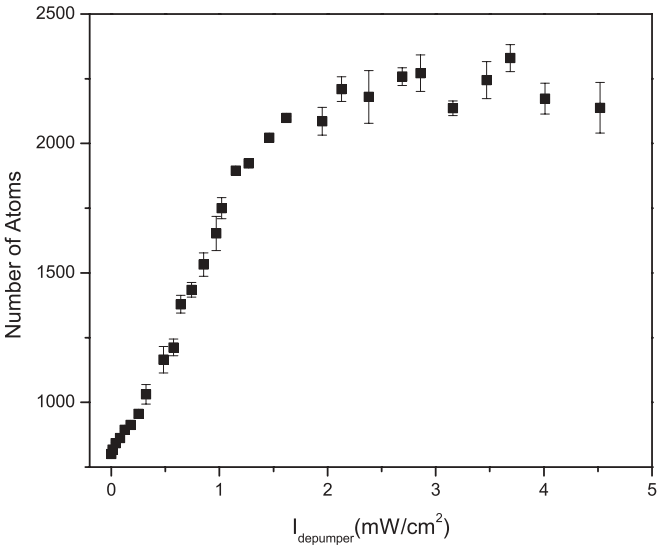


FIG. 4. Number of atoms left in the dipole trap after 100-ms trapping time as a function of the depumper intensity. The trap depth is $U_0/k_B = -1.52$ mK.

We have also investigated the dependence of the trap lifetime on the trap depth. We found that, both with and without a depumper, the trap lifetime increases for increasing trap depth. Figures 5 and 6 show our most significant measurements on the dependence of the trap lifetime on the trap depth. Figure 5 shows the atom number decay curve for the deepest trap ($U_0/k_B = -2.4$ mK) we produced with the available laser power, with and without the application of a depumper. For such a trap depth, the application of a depumper leads to a lifetime equal to $\tau = (3.6 \pm 0.4)$ s, significantly larger than the lifetime measured for $U_0/k_B = -1.78$ mK (see Fig. 3). Without the depumper, the lifetime is reduced by about one order of magnitude. The measurements of the trap lifetime as a function of the trap depth are presented in Fig. 6 for the case without the depumper. The increasing dependence of the lifetime with the trap depth is evident.

The relevant trap-loss mechanisms, which determine the trap finite lifetime, will be examined in Sec. III D.

### C. Comparison with trapping at other wavelengths

As a final point of our experiment, we compare our state-independent trap with traps at other (nonmagic) wavelengths. This allows us to verify experimentally the state-insensitive nature of the trap, and also to investigate whether certain heating mechanisms play a role in our system. We notice that for the measurements presented in this context, the dipole trap is switched off during the measurements of the number of the atoms left in the trap. This is essential in order to avoid the differential light shift associated with the (non-state-insensitive) dipole trap from affecting our measurements.

We study dipole trapping as obtained with trapping light of wavelength in the range 928–941 nm. This can be achieved by tuning the Ti:sapphire laser to the required wavelength. In order to experimentally determine the differential ac Stark shift produced by the trapping light, we take advantage of the fact that atoms in the ground-state upper hyperfine level have a shorter lifetime than atoms in the lower level, as previously discussed. We thus study the number of atoms left in the dipole trap after 100 ms as a function of the detuning from resonance of the applied depumper beam. Such a number of atoms will be maximum when the depumper is at resonance with the ac Stark-shifted $F_g = 4 \rightarrow F_e = 3$ $D_2$-line transition. Thus the depumper detuning at which the number of atoms left in the trap is maximum corresponds to the ac Stark shift of the transition.

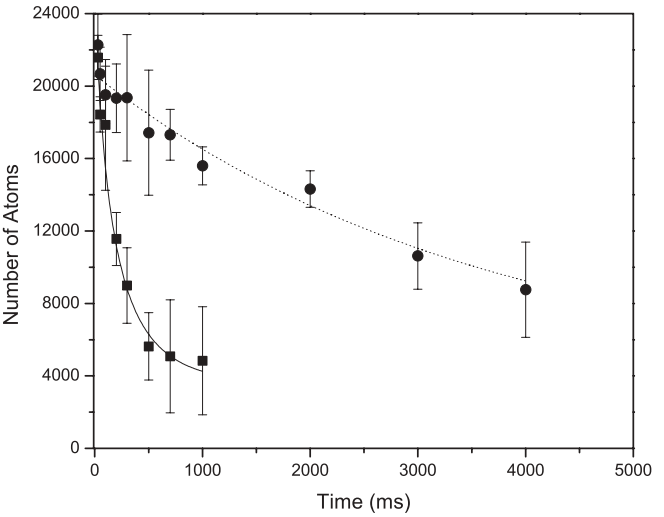


FIG. 5. Atom number decay curves for a trap depth $U_0/k_B = -2.4$ mK with (filled circles) and without (filled squares) a depumper. In the relevant case, the depumper intensity is $I_{dep} = 1.32$ mW/cm$^2$. With the application of a depumper, the effect of hyperfine-changing collisions is suppressed and the data are well fitted by a single exponential (dashed line) with decay time $\tau = (3.6 \pm 0.4)$ s. Without a depumper, hyperfine-changing collisions are very relevant, and the data can only be fitted by the full solution of Eq. (5) (solid line). The data presented here show a larger number of trapped atoms than the data in Fig. 3. This is due to the use of a higher pressure of cesium vapor.

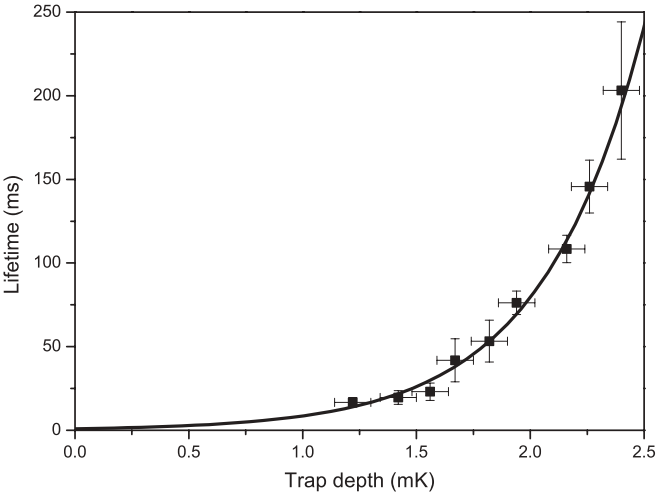


FIG. 6. Atom trap lifetime as a function of the trap depth, without the application of a depumper. The line is a guide for the eye.

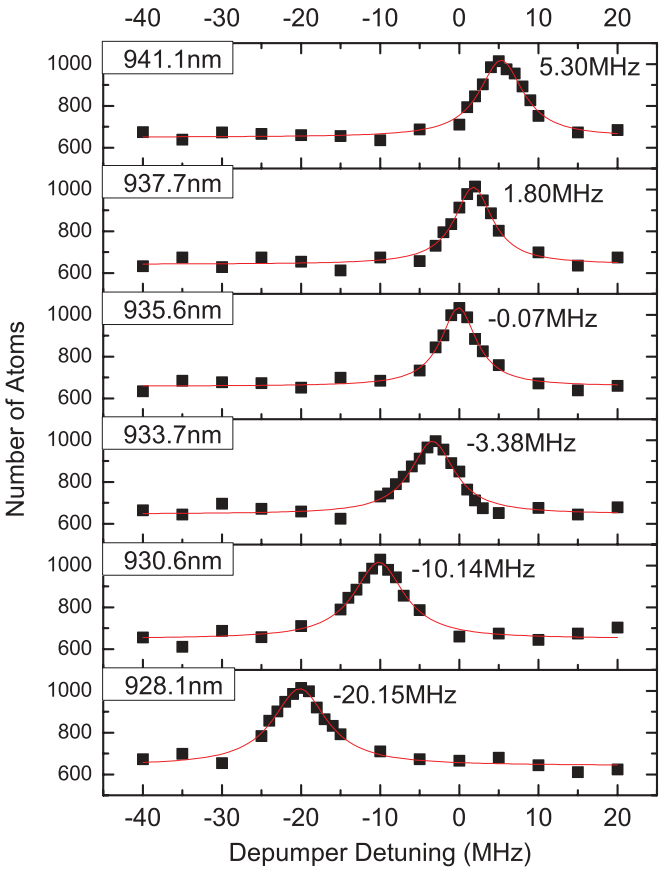


FIG. 7. (Color online) Number of atoms left in the dipole trap after 100 ms as a function of the detuning of the depumper beam. The different data sets correspond to different wavelength of the trapping light. The lines are best fits of the experimental data with a Lorentzian. The result of the fit for the Lorentzian center frequency, which corresponds to the differential ac Stark shift, is shown for each data set. For all data sets, the dipole trap depth is $U_0/k_B = -1.25$ mK.

Figure 7 shows our experimental results for the number of atoms left in the dipole trap after 100 ms as a function of the detuning of the depumper beam. Different data sets were taken for different wavelengths of the trapping beam. The maximum of each curve, as determined by fitting the data with a Lorentzian, corresponds to the differential ac Stark shift of the $F_g = 4 \rightarrow F_e = 3$ $D_2$-line transition. Figure 8 summarizes our experimental results for the differential ac Stark shift and compares them with the theoretical values. The latter ones are determined by including the contributions of the electric dipole transitions between the states $6\,S_{1/2}$, $6\,P_{1/2,3/2}$, $5D_{3/2,5/2}$, in an analogous way to Kim *et al.* [7]. In the calculation, we neglected the $(F,M)$ dependence of the light shift of the $^6P_{3/2}$ state, and report only the shift of the $D_2$-line center. Our results of Figs. 7 and 8 confirm the state-independent nature of the trapping at the magic wavelength: at $\lambda = 935.6$ nm the differential ac Stark shift is zero within the experimental error.

The last set of measurements, presented in Fig. 9, report the lifetime of the trapped atoms as a function of the wavelength of the trapping beam. Data for different depths of the trap are reported. For two of the data sets a depumper is applied, resonant with the light-shifted $F_g = 4 \rightarrow F_e = 3$ $D_2$-line transition. These data will be used to analyze the trap-loss mechanisms.

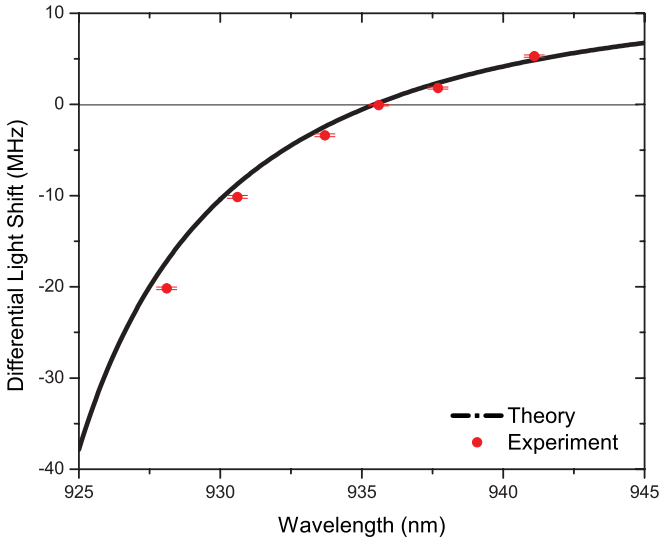


FIG. 8. (Color online) Experimental results (data points) for the differential ac Stark shift of the $F_g = 4 \rightarrow F_e = 3$ $D_2$-line transition, together with the theoretically determined value for the differential light shift of the $D_2$-line transition. The dipole trap depth is $U_0/k_B = -1.25$ mK.

### D. Trap-loss mechanisms

Several processes may limit the lifetime of a dipole trap [1,18–20]. In this section, we analyze the various loss mechanisms which may determine the observed lifetime of our trap: recoil heating, intensity fluctuations, and pointing instabilities of the trapping beam, dipole force fluctuations, and collisions with the background gas.

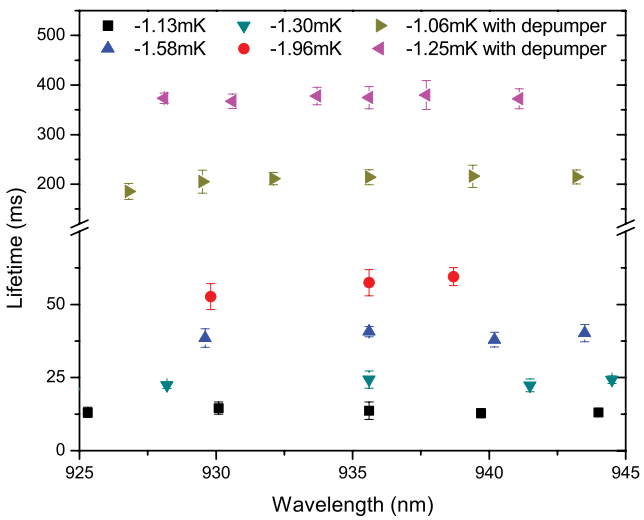


FIG. 9. (Color online) Lifetime for the atoms in the dipole trap as a function of the wavelength of the trapping beam. Different data sets correspond to different depths of the trapping potential. For the measurements of two data sets, a depumper was applied, with intensity $I_{\rm dep} = 2.72$ mW/cm$^2$.

#### 1. Recoil heating

Scattering of photons in a dipole trap leads to heating, as characterized by a recoil heating rate $\dot{Q}_{\rm rec} = 2\Gamma_{\rm sc} E_R$, where $E_R$ is the recoil energy and $\Gamma_{\rm sc}$ is the photon-scattering rate. Recoil heating causes trap losses, and the resulting trap lifetime is of the order of $U_0/\dot{Q}_{\rm rec}$ [19]. The estimated lifetime is in excess of 100 s for the entire range of wavelength considered in this work (925–945 nm, see Fig. 9), well in excess of the largest measured lifetime (~3 s). We can thus rule out recoil heating as the loss mechanism determining the lifetime of our trap.

#### 2. Dipole-trap beam-intensity fluctuations

Fluctuations in the trapping beam intensity result in fluctuations of the trap spring constant, and lead to exponential heating [19]. Quantitatively, the $e$-folding time $T_i$ (i.e., the time to increase the energy by a factor $e$ as a result of fluctuations in the spring constant in the $i = r,z$ direction), is given by $T_i^{-1} = \pi^2 \nu_i^2 S_k(2\nu_i)$ where

$$S_k(\nu) = \frac{2}{\pi}\int_0^\infty \tau \cos(\nu\tau)\langle\epsilon(t)\epsilon(t+\tau)\rangle \qquad (6)$$

is the one-sided power spectrum of the fractional fluctuation $\epsilon(t)$ in laser intensity.

We characterized the trapping beam-intensity fluctuations, and measured $S_k(2\nu_z) \simeq 1.4\times10^{-9}$ Hz$^{-1}$ and $S_k(2\nu_r) \simeq 3.9\times10^{-11}$ Hz$^{-1}$, with $\nu_z = 550$ Hz and $\nu_r = 18.5$ kHz the typical longitudinal and radial oscillation frequencies. This leads to an average $e$-folding time $\bar{T} = (T_z^{-1}/3 + 2T_r^{-1}/3)^{-1} \simeq 10$ s. For atoms prepared near the bottom of the well, the expected lifetime is in excess of the $e$-folding time, and is significantly larger than the lifetime observed in our experiment. Thus the dipole-trap beam-intensity fluctuations are not the heating mechanisms determining the trap lifetime in our experiment.

#### 3. Dipole-trap beam-pointing instabilities

Dipole-trap beam-pointing instabilities result in fluctuations of the trap center, and produce heating. For fluctuations in a given direction (say, $x$) the heating process can be characterized by a rate [19]

$$\dot{Q}_x = \frac{\pi}{2} m\omega_x^4 S_x(\omega_x), \qquad (7)$$

where $S_x$ is the one-side power spectrum of the fluctuation of the trap center in the $x$ direction. The dependence on $\omega^4$ allows us to neglect the contribution in the weakly confining longitudinal ($z$) direction.

We have characterized the point instabilities of the trapping beam by measuring, with a quadrant photodiode, the position of the beam center as a function of time. From the time series for the $x$ and $y$ components, we derived the power spectra $S_x(\omega)$ and $S_y(\omega)$. We then determined the average heating rate $\dot{Q} = (\dot{Q}_x + \dot{Q}_y)/2$ and the corresponding atom number decay time $\tau = 6.6|U_0|/\dot{Q}$. Taking $U_0 = -2.4$ mK, we found the heating relevant for the time scale of our experiment, and determined a pointing-instability atom number decay time $\tau \simeq 3.8$ s. This is of the order of the largest lifetime observed in our experiment, and shows that the beam-pointing instability is a limiting factor for the lifetime of our trap.

#### 4. Fluctuations in the dipole force

In a generic, non-state-insensitive dipole trap, changes in the internal state of the atom lead to fluctuations in the dipole force, as the dipole force associated with different atomic states is different. In a dipole trap at the magic wavelength, for the atomic transition of interest, the ground and the excited states experience the same ac Stark shift. Thus transitions between these two levels do not introduce fluctuations in the dipole force. We thus expect a decrease in momentum diffusion at the magic wavelength. Whether such a decrease produces an increase in lifetime depends on whether momentum diffusion was a limiting factor for traps at the nonmagic wavelength.

The data of Fig. 9 present the lifetime of a dipole trap versus the trapping beam wavelength. It can be seen that no evident maximum is observed at the magic wavelength. This holds both in the absence of a depumper, where hyperfine-changing collisions are the dominating loss mechanism, and with the application of a depumper. This shows that momentum diffusion produced by the fluctuations in the dipole force is not an important loss mechanism for our trap.

#### 5. Collisions with background gas

Collisions with background gas in the vacuum cell produce heating and also direct losses [21]. In a single collision an atom can be heated up and stay in the trap, or it can be expelled from the trap, depending on the collision angle and trap depth. For a collision angle larger than a critical angle, determined by the trap depth, the atom is expelled from the trap following the collision. Otherwise, for smaller angles, the atom acquires energy but stays in the trap. Thus, collisions with background gas also introduce a loss mechanism which depends on the trap depth.

By using the model developed in Ref. [21] we estimated the residual gas pressure in our chamber that would lead to the observed lifetime of $\tau = 3.6$ s for a trap depth $U_0 = -2.4$ mK. We found a value of about $3\times10^{-9}$ mbar. Such a value is within the range of pressures expected for a single-cell experiment. We thus conclude that the collisions with background gas also are a limiting factor for the lifetime of our trap.

## IV. DISCUSSION AND CONCLUSIONS

In summary, we realized and characterized a state-insensitive microdipole trap for cold cesium atoms. The use of trapping light at the magic wavelength of 935.6 nm results in the same ac Stark shift for the $^6S_{1/2}$ ground state and the $^6P_{3/2}$ excited state. By focusing a single running laser beam to a waist of $w_0 = (6.69 \pm 0.05)\,\mu$m we realized a trap with a depth of up to $U_0/k_B = -2.4$ mK. For these parameters, the scattering rate is $\Gamma_{\rm sc} \simeq 11$ s$^{-1}$, and recoil heating is negligible. By preparing the atoms in the lower hyperfine ground state, as obtained by using a depumper laser, we suppressed hyperfine-changing collisions and measured lifetimes of up to $\tau = (3.6 \pm 0.4)$ s. By analyzing the different loss mechanisms, we conclude that

the trap lifetime is limited by beam-pointing instability and collisions with the background gas.

It is interesting to compare our trap at the magic wavelength for cesium atoms with previous realizations of state-insensitive traps for the same atom [6,7]. Reference [7] reported on the realization of a single-beam trap, and demonstrated the state-insensitive nature of the trapping mechanism. That work reported a lifetime of $\tau = (350 \pm 50)$ ms for cesium atoms prepared in the lowest hyperfine level, one order of magnitude smaller than the longest lifetime reported in the present work. We attribute this difference to the smaller depth of the trap of Ref. [7], where focusing of the laser beam down to 16 $\mu$m (compared to our waist of $\simeq$6.7 $\mu$m) produced a trap depth of $-0.9$ mK (compared to our depth of $-2.4$ mK).

Reference [6] reported on state-insensitive trapping of *single* cesium atoms. Dipole trapping was realized by using the mode of a small optical cavity, with a mode waist of $\simeq$24 $\mu$m. Trap lifetimes of 2–3 s were reported for a trap depth of $-2.3$ mK. Such a lifetime, for the given trap depth, is similar to our result of $\tau \simeq 3.6$ s for a comparable trap depth of $-2.4$ mK.

Our trap, with a lifetime exceeding 3 s, is suitable for applications in atomic magnetometry. The potential of cold atoms for magnetometry is by now well recognized [22,23], and the additional use of a dipole trap allows for very long interrogation times, as required to obtain the very narrow resonances required for precision magnetometry. State-insensitive traps, such as the one discussed in this work, are suitable to implement magnetometers based on coherence between degenerate sublevels. This requires laser fields tuned to a $F_g \rightarrow F_e$ transition to prepare and probe the ground-state coherence. State-insensitive traps eliminate broadening resulting from the variation of the detuning of the preparation and probe fields which, in non-state-insensitive traps, are produced by the variation of the differential ac Stark shift across the trap as determined by the spatial variation of the light intensity. We also notice that different mechanisms (e.g., coherent population trapping or electromagnetically induced absorption [24]) may require addressing different $F_g \rightarrow F_e$ transitions. Our results show that atoms prepared in the $F_g = 3$ ground-state sublevel have a very long lifetime, so very narrow resonances can be expected for $F_g = 3 \rightarrow F_e = 2,3,4$. On the contrary, for atoms prepared in the $F_g = 4$ ground-state sublevel, we found that the hyperfine-changing collision limited the trapped atoms' lifetime, thus setting a limit for the use of $F_g = 4 \rightarrow F_e = 3,4,5$ transitions for the production of interaction-time-limited narrow resonances. However, such a limit can be circumvented by using a magic optical lattice, as introduced in the context of atomic clocks [5]. The loading of no more than one atom per site is expected to suppress collisional events, thus increasing the trapped atom lifetimes, and allowing the use of $F_g = 4 \rightarrow F_e = 3,4,5$ for the production of very narrow resonances, which is of interest for magnetometry.

## ACKNOWLEDGMENTS

This work was funded by EPSRC. We thank Y. Ovchinnikov for useful discussions.

[1] R. Grimm, M. Weidemüller, and Y. Ovchinnikov, Adv. At. Mol. Opt. Phys. **42**, 95 (2000).
[2] T. Ido, Y. Isoya, and H. Katori, Phys. Rev. A **61**, 061403(R) (2000).
[3] H. Katori, M. Takamoto, V. G. Pal'chikov, and V. D. Ovsiannikov, Phys. Rev. Lett. **91**, 173005 (2003).
[4] M. Takamoto and H. Katori, Phys. Rev. Lett. **91**, 223001 (2003).
[5] M. Takamoto, F.-L. Hong, R. Higashi, and H. Katori, Nature (London) **435**, 321 (2005).
[6] J. McKeever, J. R. Buck, A. D. Boozer, A. Kuzmich, H.-C. Nägerl, D. M. Stamper-Kurn, and H. J.-Kimble, Phys. Rev. Lett. **90**, 133602 (2003).
[7] J. Y. Kim, J. S. Lee, J. H. Han, and D. Cho, J. Korean Phys. Soc. **42**, 483 (2003).
[8] J. Ye, H. J. Kimble, and H. Katori, Science **320**, 1734 (2008).
[9] P. Rosenbusch, S. Ghezali, V. A. Dzuba, V. V. Flambaum, K. Beloy, and A. Derevianko, Phys. Rev. A **79**, 013404 (2009).
[10] V. V. Flambaum, V. A. Dzuba, and A. Derevianko, Phys. Rev. Lett. **101**, 220801 (2008).
[11] K. Beloy, A. Derevianko, V. A. Dzuba, and V. V. Flambaum, Phys. Rev. Lett. **102**, 120801 (2009).
[12] C. G. Townsend, N. H. Edwards, K. P. Zetie, C. J. Cooper, J. Rink, and C. J. Foot, Phys. Rev. A **53**, 1702 (1996).
[13] W. Alt, Optik **113**, 3 (2002).
[14] S. Friebel, C. D'Andrea, J. Walz, M. Weitz, and T. W. Hänsch, Phys. Rev. A **57**, R20 (1998).
[15] S. Balik, A. L. Win, and M. D. Havey, Phys. Rev. A **80**, 023404 (2009).
[16] C. Salomon *et al.*, unpublished data reported in Fig. 4 of Ref. [1].
[17] S. J. M. Kuppens, K. L. Corwin, K. W. Miller, T. E. Chupp, and C. E. Wieman, Phys. Rev. A **62**, 013406 (2000).
[18] T. A. Savard, K. M. O'Hara, and J. E. Thomas, Phys. Rev. A **56**, R1095 (1997).
[19] M. E. Gehm, K. M. O'Hara, T. A. Savard, and J. E. Thomas, Phys. Rev. A **58**, 3914 (1998).
[20] S. Bali, K. M. O'Hara, M. E. Gehm, S. R. Granade, and J. E. Thomas, Phys. Rev. A **60**, R29 (1999).
[21] H. C. W. Beijerinck, Phys. Rev. A **61**, 033606 (2000).
[22] M. L. Terraciano, M. Bashkansky, and F. K. Fatemi, Phys. Rev. A **77**, 063417 (2008).
[23] A. Wojciechowski, E. Corsini, J. Zachorowski, and W. Gawlik, Phys. Rev. A **81**, 053420 (2010).
[24] F. Renzoni, W. Maichen, L. Windholz, and E. Arimondo, Phys. Rev. A **55**, 3710 (1997); F. Renzoni, C. Zimmermann, P. Verkerk, and E. Arimondo, J. Opt. B: Quantum Semiclass. Opt. **3**, S7 (2001).